



ELSEVIER

International Journal of Mass Spectrometry 184 (1999) 25–38



# Gas-phase basicities of deprotonated matrix-assisted laser desorption/ionization matrix molecules

K. Breuker, R. Knochenmuss, R. Zenobi\*

*Department of Chemistry, Swiss Federal Institute of Technology (ETH), Universitätstrasse 16, CH-8092 Zürich, Switzerland*

Received 21 August 1998; accepted 2 October 1998

## Abstract

The gas-phase basicities (GB) of eight matrix-assisted laser desorption/ionization (MALDI) matrix anions were determined using a modified bracketing method. Reference anions were generated by laser desorption from a newly developed two-phase liquid/solid mixed matrix, allowing measurements at a well defined temperature (299 K) and under low pressure conditions. The most basic matrix anion found was that of 3-aminoquinoline (GB = 1451 kJ/mol) and the least basic was the 2,4,6-trihydroxyacetophenone anion (GB = 1324 kJ/mol). Consequences for the MALDI process are discussed with respect to matrix ion formation, oligonucleotide and protein analysis. Ground-state proton transfer plume reactions between matrix anions and analyte molecules were found to be energetically favorable in many cases. (*Int J Mass Spectrom* 184 (1999) 25–38) © 1999 Elsevier Science B.V.

*Keywords:* Matrix-assisted laser desorption/ionization; Matrix; Bracketing; Gas-phase basicity; Oligonucleotides

## 1. Introduction

Although matrix-assisted laser desorption/ionization (MALDI) [1] has become a widespread ionization technique successfully applied in the analysis of biological, biochemical, and industrial samples, neither matrix nor analyte ionization is fully understood yet. Here we present fundamental thermochemical MALDI matrix properties which are relevant to the MALDI process.

Proton transfer reactions have been suggested as the basic mechanism for analyte ionization in both positive [2] and negative [3] polarity. Bökelmann and co-workers studied the dynamic parameters of ion

formation in MALDI [4]. They observed a significant quenching of matrix ions in areas of high peptide ion density, and suggest gas-phase proton transfer from matrix ions to analyte molecules. Analysis of time-of-flight profiles of bovine insulin cluster ions carried out by Kinsel and co-workers [5] strongly suggests a two-component model for MALDI ion formation. The ion profiles were best described with one fraction of analyte ions that are formed promptly, and another fraction of about equal intensity that is formed with a delay of about 30 ns. For the delayed reactions, it seems unlikely that excited state chemistry plays an important role because the lifetime of excited states is usually shorter than 30 ns. In a recent study, Jørgensen and co-workers observed a correlation between the proton affinity of the matrix used and the formation of multiply charged protonated analyte ions

\* Corresponding author.

[6], giving further evidence that proton transfer plume reactions are of great importance for analyte ionization.

Several groups have reported ground-state proton affinities (PA) and gas-phase basicities (GB) of matrix molecules [6–9] and neutral fragments thereof [8]. To date, a lack of data on negatively charged matrix species has prevented further insight into possible deprotonation mechanisms.

The gas-phase basicity of an anion  $(M - H)^-$ ,  $GB((M - H)^-)$ , is the negative of the free energy change  $\Delta G$  of the protonation reaction



usually defined at 298 K.

Techniques that have been used to establish relative gas-phase basicities are the equilibrium, kinetic, and bracketing methods. These have been reviewed and discussed by Harrison [10].

With the equilibrium method [11], the gas-phase basicity of a test base can be determined by measuring either the equilibrium constant or the rate constants for the forward and reverse reactions of a proton transfer between the test base and a reference base with known GB. Additionally, by determination of the equilibrium constant as a function of temperature, the proton affinity ( $-\Delta H$  of a protonation reaction) can be derived. An essential prerequisite of this method is, of course, that equilibrium is established, and moreover, that equilibrium concentrations of both ionic and neutral species involved in the proton transfer reaction can be determined accurately. The equilibrium method can therefore only be applied if all species under investigation are sufficiently volatile, which is typically not the case for molecules used in MALDI.

Because proton-bound cluster ions can in many cases be easily prepared by desorption/ionization techniques such as fast atom bombardment (FAB), MALDI or electrospray ionization (ESI), the kinetic method is ideal for the study of nonvolatile compounds. With this method, the fragmentation of proton-bound heterodimer ions, consisting of a reference and a test compound, is studied [12]. In order to

dissociate the weakly bound cluster species, a technique such as collisional or infrared multiple photon (IRMP) activation needs to be employed [13,14]. Assuming equal detection efficiencies, the ratio of fragment ion signals will then equal the ratio of rate constants for the competing dissociation channels, from which gas-phase basicities and proton affinities can be derived.

In the bracketing method [15], abrupt changes in reactivity with reference compounds are used to assign gas-phase basicities. Fast reactions are considered as exoergic and slow reactions are classified as endoergic [10]. By reacting a test species with a variety of reference substances, its gas-phase basicity can be bracketed. Reaction efficiencies (RE) can be used to distinguish fast and slow reactions. These are defined as the ratio of the experimental rate constant  $k_{\text{exp}}$  and either the collision rate constant  $k_{\text{coll}}$  or a theoretical rate constant  $k_{\text{ADO}}$  [16–18] obtained from average dipole orientation theory [19].  $RE = 1$  indicates an exoergic, and  $RE = 0$  an endoergic reaction. A RE of unity denotes the situation where every collision results in a proton transfer. As the RE decreases, which is the case in near-thermoneutral reactions, the number of collisions required for proton transfer to occur increases. A RE of zero means that independent of the number of collisions, proton transfer will not proceed. However, values for  $k_{\text{exp}}$ ,  $k_{\text{coll}}$ , and  $k_{\text{ADO}}$  can only be determined with relatively low precision. For example, experimental rate constants were reproducible to no better than 25% (relative standard deviation) in a study carried out by McKiernan and co-workers [18]. Together with the fact that collision rate constants also can only be determined with limited accuracy, relatively large errors for the reaction efficiencies can result. This is reflected in the calculated reaction efficiencies, which then can have unphysical values significantly larger than unity (for example 1.78 was found in [17]). The criterion used to decide whether a reaction is considered exoergic or endoergic was if the reaction efficiency is larger or smaller than either 0.5 [17] or 0.1 [18], respectively. Assigning a bracketing point on the basis of reaction efficiencies is therefore difficult

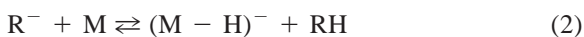
when reaction efficiencies can only be determined with such low precision.

Bouchoux and co-workers discussed the relationship between the kinetics and the thermochemistry of gas-phase proton transfer reactions and suggested a more facile method for determining GB values [16]. All data obtained in a bracketing series can be exploited to define a fitting function based on a steady-state assumption and transition state theory. From this function, the GB of the species under investigation can be derived with a precision of  $\pm 5$  kJ/mol.

Here we show how GB values can be deduced from relative ion abundances rather than from kinetics, provided that the abundances are probed after a sufficiently long reaction delay. It was empirically observed that near-equilibrium conditions were established after a certain reaction time, justifying a theoretical treatment based on equilibrium and transition state theory. Applying this method for a series of reference bases and fitting the complete data set yields reliable GB values for the anions under study.

### 1.1. Theoretical treatment

The neutral matrix molecules (M) were allowed to undergo reactions with reference bases ( $R^-$ ) of known gas-phase basicities. For the reaction



the equilibrium constant  $K_{eq}$  is given by

$$K_{eq} = \frac{[(M - H)^-][RH]}{[R^-][M]} \quad (3)$$

By stoichiometry, the concentration of deprotonated matrix molecules is equal to the concentration of protonated reagent ions RH at any stage of the reaction, including equilibrium. If the total ion intensities in each spectrum are normalized, we can write the equilibrium constant for reaction (2) as:

$$K_{eq} = \frac{x^2}{(1 - x) \cdot M_0} \quad (4)$$

where  $x$  is the normalized  $(M - H)^-$  concentration,

$$x = \frac{[(M - H)^-]}{[(M - H)^-] + [R^-]} \quad (5)$$

and  $M_0$  stands for the relative concentration of neutral matrix molecules,

$$M_0 = \frac{[M]}{[(M - H)^-] + [R^-]} \quad (6)$$

Under equilibrium conditions, the equilibrium constant and the free energy change of reaction (2) are related through

$$\Delta G = -RT \ln K_{eq} \text{ or } K_{eq} = \exp[-\Delta G/RT] \quad (7)$$

The free energy change of reaction (2) is given by the difference in gas-phase basicities of product and educt ions:

$$\Delta G = GB((M - H)^-) - GB(R^-) \quad (8)$$

Because ion intensities have been normalized, the value of  $x$  will be between 0 and 1,  $x \in [0, 1]$ , and it follows that  $K_{eq} \in [0, \infty]$ . This makes  $K_{eq}$  an impractical parameter for data visualization, so the experimental data were instead plotted as  $R_k$  values defined as follows:

$$R_k = \frac{1}{1 + M_0 \cdot K_{eq}} = \left[ 1 + \frac{x^2}{1 - x} \right]^{-1} \quad (9)$$

This has the advantageous properties that if  $x$  approaches 0, the  $R_k$  value will approach 1 and if  $x$  approaches 1,  $R_k$  will approach 0. The  $R_k = 1$  value corresponds to no product ion yield, and the  $R_k = 0$  value corresponds to 100% product ion yield. Using the expression for  $K_{eq}$  in Eq. (7), and expanding  $\Delta G$  as in Eq. (8), Eq. (9) gives the fit function to derive  $GB((M - H)^-)$  from  $R_k$  for a series of test bases:

$$R_k(GB(R^-)) = \left[ 1 + M_0 \exp \left[ -\frac{GB((M - H)^-) - GB(R^-)}{RT} \right] \right]^{-1} \quad (10)$$

Besides the desired  $(M - H)^-$  ion,  $RM^-$  heterodimer ions were detected in many cases, especially for near-thermoneutral deprotonation reactions. Because proton transfer and not adduct formation is of interest here, the intermediate  $RM^-$  is considered as unreacted material formally equivalent to  $R^-$ . Therefore the term  $[R^-]$  in Eq. (2), (3) includes the measured  $RM^-$  concentration.

The formation of intermediate ions was also observed by McKiernan [18] and Wu [17] in bracketing experiments in positive mode. Both groups defined the reaction efficiencies as rate ratios and considered the intermediate as unreacted material. For a data analysis as suggested by Bouchoux and co-workers [16], this is somewhat contradictory, because the rate-ratio data treatment is based on a steady-state approximation, meaning that it assumes a highly reactive intermediate. With our equilibrium approach, we also do not treat the intermediate as an individual species, but we assume equilibrium conditions which allow for its formation.

In order to exactly determine  $M_0$ , both the absolute ion and neutral concentrations need to be measured accurately. The latter is constant for a given matrix, but vapor pressures are not known for these compounds. Employing the electron filament for neutral density determination would increase the temperature of the cell and the metal target supporting the solid matrix, resulting in increased sublimation and an overestimation of the partial matrix pressure compared to the GB measurements with no filament. The relative matrix concentration  $M_0$  in Eq. (10) was therefore estimated from ion densities and exoergic reaction rates using collision theory. Judging from signal intensities, estimated instrument sensitivity, and absence of space-charge effects, a reasonable value for the number of ions trapped in the ICR cell was  $10^4$ , equivalent to an ion density of  $1.22 \cdot 10^{11} \text{ L}^{-1}$  in the active cell volume of  $8.2 \cdot 10^{-8} \text{ L}$ . The latter is given by the ICR orbital radius of an  $m/z = 100$  ion at thermal energies and 4.7 T, the trapping potential of  $-1 \text{ V}$ , and the cell dimensions. With the assumed ion density  $\rho = 1.22 \cdot 10^{11} \text{ L}^{-1}$  and an estimated collision cross section  $\sigma$  of  $10^{-18} \text{ m}^2$  [20], we can calculate  $M_0$  from collision theory. For reac-

tions that proceed with unit efficiency, the rate of change in  $R^-$  concentration,  $[R^-]$ , is given by the collision density  $Z$  [21],

$$Z = -d[R^-]/dt = \sigma \sqrt{8kT/\pi\mu} \cdot [R^-] \cdot [M] \quad (11)$$

where  $[M]$  is the matrix concentration,  $T$  the temperature,  $k$  the Boltzmann constant, and  $\mu$  the reduced mass of reference anion and matrix molecule. Assuming first-order kinetics and because rates were obtained from normalized reference ion intensities  $[R^-]_n$  (where the normalization factor was the same as used for normalization of the matrix concentration), we can write (11) as:

$$k_{\text{exp}} = \sigma \sqrt{8kT/\pi\mu} \cdot \rho \cdot M_0 \quad (12)$$

from which we can extract  $M_0$  values. The rate constants  $k_{\text{exp}}$  were obtained from the kinetics of highly exoergic reactions, where every collision results in proton transfer. For all matrices except for *para*-nitroaniline and 2,5-dihydroxybenzoic acid,  $M_0$  values between 1 and 10 were obtained. For *para*-nitroaniline, a higher value of 48 was determined, corresponding to the significantly higher vapor pressure of *para*-nitroaniline. On the other end of the scale, the  $M_0$  value for 2,5-dihydroxybenzoic was found to be 0.65. Partial matrix pressures in the cell volume can then be back calculated to range from  $3 \times 10^{-9}$  to  $2 \times 10^{-7}$  mbar.

The  $M_0$  values from the kinetic analysis were used in the fitting functions. As part of the error analysis, two extreme cases were considered. In the first case, a small ion number of  $10^3$  was hypothesized together with a tenfold higher partial matrix pressure than found above, giving a relative matrix concentration of  $100 \cdot M_0$ . In the second case, the ion number was assumed to be high ( $10^5$ ), and the partial matrix pressure was taken an order of magnitude lower, resulting in a relative matrix concentration of  $0.01 \cdot M_0$ . These conservative bounds for  $M_0$  span four orders of magnitude and far exceed possible uncertainties resulting from ion-dipole interactions, which can enhance maximum reaction rate constants

by at most a factor of 2–4 [22]. A covariance analysis showed that the matrix GB error derived from the reference GB uncertainty was much smaller than the matrix GB error because of these conservative bounds for  $M_0$ .

## 2. Experimental

Experiments were performed utilizing a Fourier transform ion cyclotron resonance (FTICR) mass spectrometer with a 4.7 Tesla superconducting magnet (Bruker, Fällanden, Switzerland). The laboratory-built vacuum system comprised a cylindrical ion cell and a sample transfer device for insertion of solid material. The RF electronics and Odyssey data acquisition system were from Finnigan (Finnigan FT/MS, Madison, WI, USA). For laser desorption, a Nd:YAG laser (Continuum, Minilite ML-10) operated at 355 nm was employed. The typical laser irradiance used was  $4 \cdot 10^6$  W/cm<sup>2</sup> or less. Reference ions were trapped within a  $-1$  V static potential and allowed to axialize for 5 s prior to stored waveform inverse Fourier transform (SWIFT) isolation, a variable reaction delay, chirp excitation, and subsequent detection. In a few cases, the cooling delay was reduced to as little as 1 s. This was necessary for highly exothermic reactions ( $\Delta GB > 40$  kJ/mol) together with relatively high matrix vapor pressures. These reactions then proceeded so fast that the reference anions would otherwise be reacted away during the cooling period.

Before starting a series of bracketing experiments, the vacuum system was cleaned with a bakeout procedure. After the system cooled to room temperature ( $299 \pm 1$  K), a solid sample of the MALDI matrix under investigation was inserted into the main chamber. The sublimed material was then allowed to adsorb on the vacuum system and cell walls during a one hour period, resulting in a good wall coverage. For each reference base, a target carrying both solid matrix material which was placed on the outer rim of the target and a two-phase sample for reference anion generation (placed in the center) was prepared. This target was then positioned about 15 mm from one trapping plate of the cell. Tetrabutylammonium salts (TBA hydrogen sulfide, TBA cyanide, TBA acetate,

TBA cyanate, TBA thiophenolate, TBA benzoate, TBA chloride, TBA bromide, TBA nitrate, TBA rhodanide, TBA methanesulfonate, TBA iodide, TBA hydrogen sulfate, TBA trifluoromethanesulfonate) were purchased from Fluka (Buchs, Switzerland). Silicon particulates (325 mesh, corresponding to 45  $\mu$ m diam.) were purchased from Aldrich (Buchs, Switzerland). 3-aminoquinoline, *para*-aminophenol, 2-amino-3-hydroxypyridine, 4-hydroxybenzoic acid, nicotinic acid and 2,5-dihydroxybenzoic acid were from Fluka. *Para*-nitroaniline, 2-amino-5-nitropyridine, 3-hydroxypicolinic acid and 2,4,6-trihydroxyacetophenone were from Aldrich.

## 3. Reference anion generation

In conventional bracketing experiments, reference ions are produced by electron bombardment of a volatile gas which is introduced through a pulsed valve. This method has substantial disadvantages. First, the gas pulse is detrimental to ICR working conditions. Besides the desired gas, impurities from former experiments may also still be present in the inlet line and can lead to erroneous results. Second, the hot electron filament, which is usually located close to the ICR cell, causes a temperature gradient along the cell volume in which the ion/molecule reactions take place. The resulting temperature uncertainty can lead to incorrect thermochemical data. Third, reference ions such as protonated or deprotonated species are commonly generated by chemical gas-phase reactions following an electron impact event, as there are radical ion formation and subsequent self-protonation/self-deprotonation or protonation/deprotonation via an additional precursor ion. These reactions can be complicated by competing reactions such as electron transfer and clustering. Desorption of preformed reference anions [23] avoids all such complications and was found to be a straightforward technique. Defined (low) temperature, generation of only the desired ion species and low pressure conditions are the main advantages.

The anions were laser desorbed from a liquid/solid binary matrix consisting of a concentrated TBA salt solution and silicon particulates to absorb the laser

energy [23]. Because this matrix almost exclusively yields the desired reference anions, the SWIFT isolation waveform was primarily used to eject matrix ions which can already form during the cooling period, rather than to eject species formed upon laser desorption.

## 4. Results and discussion

### 4.1. Bracketing results

The ion/molecule reaction products detected were either deprotonated matrix anions ( $M - H$ )<sup>-</sup>,  $MR$ <sup>-</sup> heterodimer ions, or both species simultaneously. Fig. 1 illustrates typical spectra obtained in bracketing experiments after a 30 s reaction time. Depending on their gas-phase basicities, the various reference anions yield different types of product ions when reacting with the matrix molecules. As shown in the upper trace, the methanesulfonate anion is depleted solely by complex formation with the MALDI matrix 2-amino-5-nitropyridine (2A5NP), so we conclude that the proton transfer reaction is endoergic. The benzoate anion forms both complex ions and deprotonated matrix, indicating a near-thermoneutral proton transfer reaction (see middle trace). In the lower trace, a pure deprotonation reaction between the thiophenolate anion and 2A5NP is shown, which we classify as exoergic. The relative yield of deprotonated matrix increases with increasing reference anion basicity.

We observed that near-equilibrium conditions were established after reaction times of about 10 s or less, as is illustrated in Fig. 2. The kinetic plot shows the relative intensities of the reference anion  $CNO$ <sup>-</sup>, deprotonated *para*-nitroaniline ( $PNA - H$ )<sup>-</sup>, and  $(PNA + CNO)$ <sup>-</sup> complex ions, respectively. After relatively rapid changes during the first 10 s, the normalized ion abundances become almost constant. The near-equilibrium conditions allow us to treat the data as described above. With this method, we do not assign a “bracketing point” between two reference bases, which is obviously difficult when near-thermoneutral reactions occur, but take into account the bracketing results of all reference anions with a given

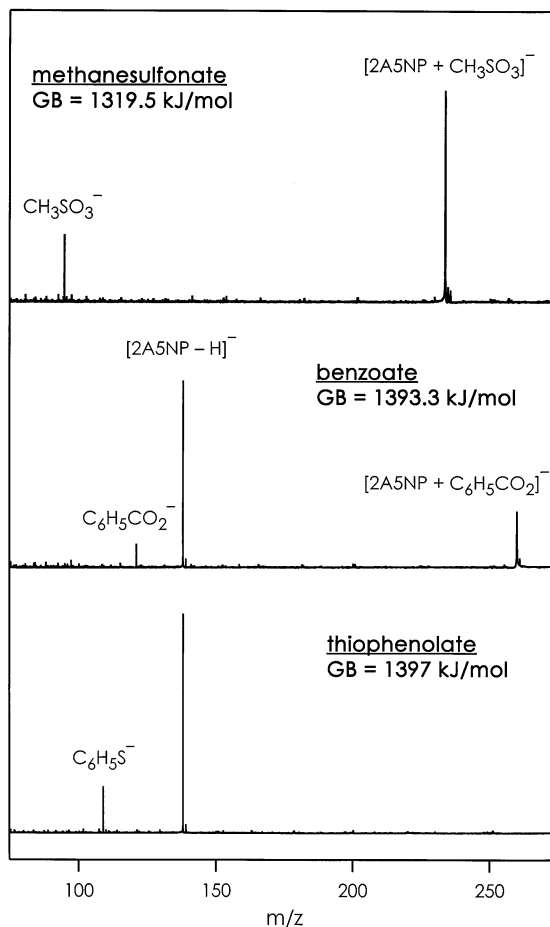


Fig. 1. Typical mass spectra obtained in bracketing experiments, illustrated for reactions of reference anions with the MALDI matrix 2-amino-5-nitropyridine (2A5NP). The reaction time was 30 s. Upper trace: Adduct ion formation with 2A5NP depletes the methanesulfonate anion, and no deprotonated matrix is observed. Middle trace: the benzoate anion forms both adduct ions and deprotonated 2A5NP. Lower trace: the thiophenolate anion reacts by deprotonating 2A5NP, whereas the adduct species is not observed. The relative yield of deprotonated matrix is correlated with the reference anion basicity, increasing from top to bottom.

matrix molecule. The reference anion GB literature values were from the National Institute of Standards and Technology database [24,25], and in the case where more than one value was listed, average values were used, as summarized in Table 1. Literature values with errors larger than 20 kJ/mol were disregarded.

The reactions of various reference anions with



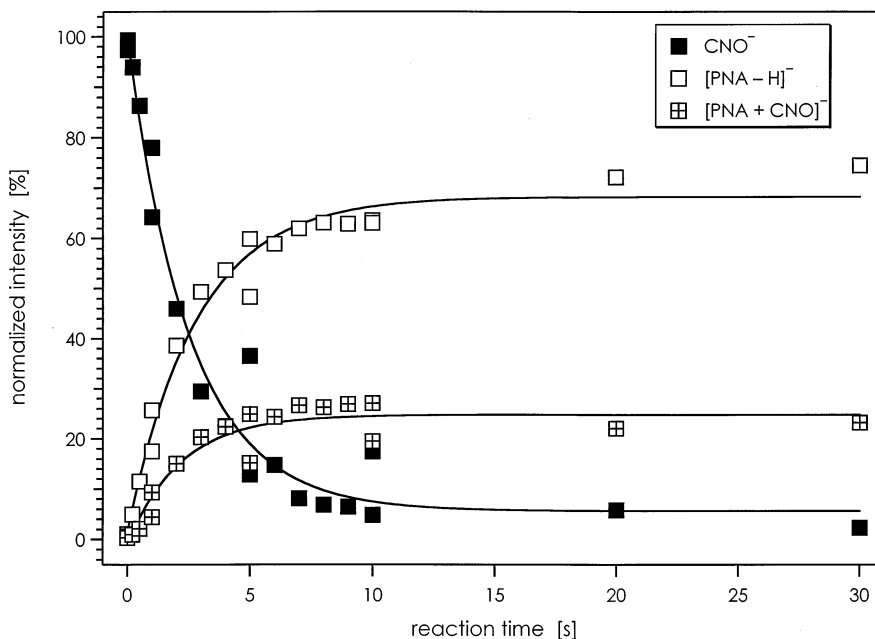


Fig. 2. Kinetic plot of the reaction between cyanate ( $\text{CNO}^-$ ) and *para*-nitroaniline (PNA). The solid lines are exponential fit functions. Near-equilibrium conditions were established after about 7 s reaction time.

PNA were monitored as a function of time, and from the relative ion abundances,  $R_k$  values were calculated. Using Eq. (10), GB values at 299 K were obtained. A nonlinear, least-square fitting procedure was employed for data evaluation. Experimental data were weighted with the reference base GB errors in the fitting procedure. Experimental data and the corresponding  $R_k$  fit functions are depicted in Fig. 3 for reaction times of 1, 5, and 30 s. After a relatively rapid change of  $R_k$  values during the first seconds, which corresponds to nonequilibrium conditions, no further significant change can be observed. The  $R_k$  values after 10, 20, and 30 s reaction times are almost undistinguishable. The same is true for the derived gas-phase basicities, as illustrated in Fig. 4. The data in Fig. 4 reflect the kinetics of the various reactions and were fitted with an exponential function. The gas-phase basicity of the *para*-nitroaniline anion ( $\text{PNA} - \text{H}^-$ ) determined with this method is  $1410.6 \pm 11.5$  kJ/mol, which is in very good agreement with the literature value of  $1407.0 \pm 8.4$  kJ/mol [23].

In order to further validate the method, we determined the gas-phase basicities of *para*-aminophenol (pAP) and 4-hydroxybenzoic acid (HBA). These molecules are not used as MALDI matrices, but are chemically similar to some matrices and literature values are available. The  $(\text{HBA} - \text{H})^-$  anion basicity found,  $1378.0 \pm 11.5$  kJ/mol, is in excellent agreement with the literature value of  $1376.0 \pm 8.4$  kJ/mol [24]. For *para*-aminophenol, we determined a GB value of  $1438.3 \pm 11.5$  kJ/mol. The literature value is larger,  $1450 \pm 8.4$  kJ/mol [24], but within the errors still in agreement. Literature values and our data obtained from the analysis of  $R_k$  values are summarized in Table 2.

In a few cases, the deprotonated matrix molecule was found to form a  $(2\text{M} - \text{H})^-$ -type complex by attachment of an additional matrix molecule. This ion appeared only slowly and was always minor in abundance for reaction times up to 30 s. It was treated in the analysis as a  $(\text{M} - \text{H})^-$ -type matrix anion.

2,5-dihydroxybenzoic acid (DHB) and 2,4,6-trihydroxyacetophenone (THAP) were the only matrices

Table 1  
Reference anion gas-phase basicities

Reference anion $X^-$	GB( $X^-$ ) [kJ/mol]	GB <sub>average</sub> ( $X^-$ ) [kJ/mol]
$HS^-$	$1443 \pm 8.4^a$	$1444.5 \pm 8.4$
	$1446 \pm 8.4^a$	
$CN^-$	$1427 \pm 8.8^a$	$1432.5 \pm 8.6$
	$1438 \pm 8.4^a$	
$CH_3CO_2^-$	$1427 \pm 8.4^a$	$1428.7 \pm 8.4$
	$1429 \pm 8.4^a$	
$CNO^-$	$1430 \pm 8.4^a$	$1407.5 \pm 12.2$
	$1400 \pm 16^a$	
	$1415 \pm 8.4^a$	
$C_6H_5S^-$	$1397 \pm 8.4^a$	$1397 \pm 8.4$
$C_6H_5CO_2^-$	$1393 \pm 8.4^a$	$1393.3 \pm 8.4$
	$1393 \pm 8.4^a$	
	$1394 \pm 8.4^a$	
$Cl^-$	$1373.6 \pm 8.4^b$	$1373.6 \pm 8.4$
$Br^-$	$1331.8 \pm 0.84^a$	$1331.4 \pm 4.6$
	$1331 \pm 8.4^a$	
$NO_3^-$	$1329.7 \pm 0.84^a$	$1329.7 \pm 0.84$
$CNS^-$	$1329 \pm 5.9^a$	$1329 \pm 5.9$
$CH_3SO_3^-$	$1318 \pm 8.4^a$	$1319.5 \pm 8.4$
	$1321 \pm 8.4^a$	
$I^-$	$1293.7 \pm 0.84^a$	$1293.7 \pm 0.84$
$HSO_4^-$	$1265 \pm 10^a$	$1265 \pm 10$
$CF_3SO_3^-$	$1253 \pm 8.4^a$	$1251.5 \pm 9.2$
	$1250 \pm 10^a$	

<sup>a</sup> From [24].

<sup>b</sup> From [25].

investigated here for which a 30 s reaction delay was not sufficiently long to determine the corresponding anion GBs. The exoergic reactions with DHB were only complete after a 90 s reaction time. On this extended timescale, the formation of  $(2M - H)^-$ -type homodimer ions became significant. The ratio of  $(DHB - H)^-$  and  $(2DHB - H)^-$  ions after a 90 s reaction time was about one. We regarded the homodimer ion as deprotonated matrix. With this assumption, the derived gas-phase basicity of  $(DHB - H)^-$  is  $1329.4 \pm 11.5$  kJ/mol. The bromide and nitrate anions reacted with DHB both by deprotonation and complex formation, whereas the rhodanide anion reacted only by heterodimer complex formation. From a qualitative bracketing viewpoint, then, the derived gas-phase basicity of 1329.4 kJ/mol is therefore reasonable. However, on this longer timescale some departure from equilibrium cannot be ruled out because neutral product molecules will

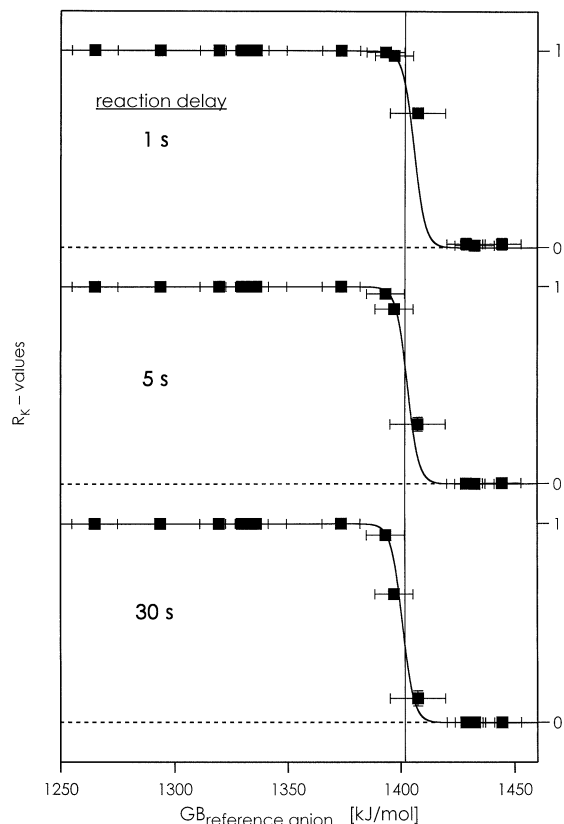


Fig. 3.  $R_k$  values as a function of reference anion basicity for reactions of *para*-nitroaniline (PNA) with several reference anions (hydrogen sulfide, cyanide, acetate, thiophenolate, benzoate, chloride, bromide, nitrate, rhodanide, methanesulfonate, iodide, hydrogen sulfate). Reaction times were 1, 5, and 30 s, respectively. Solid lines are fit functions of the type (10) as discussed in the text for 299 K and a relative matrix concentration  $M_0 = 48$ . The vertical reference line at  $GB = 1402$  kJ/mol helps to see the shifting of fit functions towards lower GB with increasing reaction time. The shift during the first 5 s was much larger than the shift between 5 and 30 s.

slowly be pumped out of the cell volume, driving the reaction further towards products.

For THAP, the observed reactions were even slower. After a 30 s reaction delay, the product ion yield was only about 20%. The bromide and rhodanide ( $CNS^-$ ) anion both reacted by formation of  $(THAP - H)^-$  and heterodimer complex anions in approximately equal abundance. The nitrate anion yielded exclusively  $(THAP - H)^-$  ions, whereas the methanesulfonate exclusively formed heterodimer an-



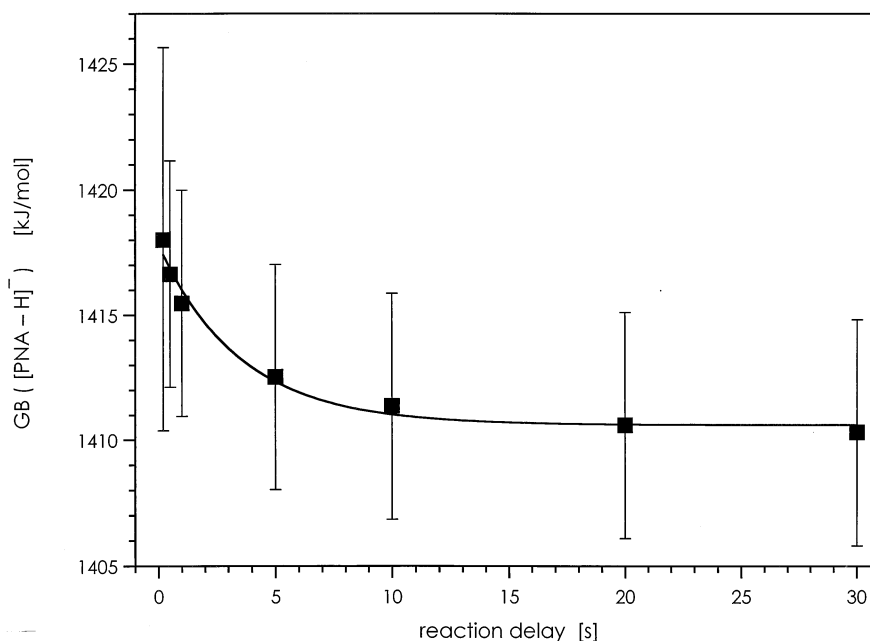


Fig. 4. Derived gas-phase basicities as a function of reaction time. After a relatively rapid initial decrease, the GB clearly approaches a limit value. The solid line is an exponential fit function with an asymptotic value of 1410.6 kJ/mol. Error bars show the error in GB obtained from a covariance analysis.

ions. THAP was the only matrix here which was deprotonated by the rhodanide anion. The GB of the (THAP - H)<sup>-</sup> anion was therefore determined by bracketing between rhodanide (GB = 1329 kJ/mol) and methanesulfonate (GB = 1319.5 kJ/mol), giving rise to a (THAP - H)<sup>-</sup>-gas-phase basicity of  $1324.3 \pm 7.1$  kJ/mol. The relative order of (DHB - H)<sup>-</sup> and (THAP - H)<sup>-</sup> anion basicities was confirmed in a proton transfer experiment. The (DHB - H)<sup>-</sup> anion reacted with THAP in a pure deprotonation reaction.

The method described here could not be utilized for determination of anion GBs of sinapic acid, ferulic acid, and 2-(4-hydroxyphenylazo)-benzoic acid (HABA), because these matrices were found to have insufficient vapor pressure. For example, the reaction between acetate and ferulic acid, which by analogy to the other carboxylic acids can reasonably be assumed to be exoergic, was far from completion even after 1000 s reaction time.

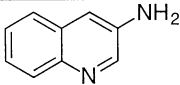
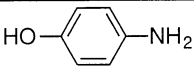
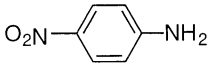
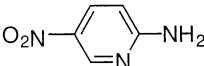
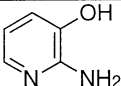
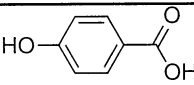
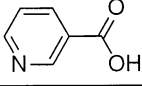
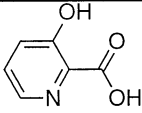
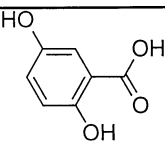
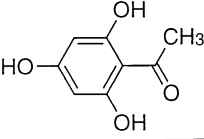
## 5. Consequences for MALDI

### 5.1. Matrix ion generation

Protonated and deprotonated matrix ions have been suggested to act as reagents for analyte ionization, but the mechanism by which matrix ions are created is still under investigation. Karbach and Knochenmuss recently measured the ionization potential of DHB molecules to be 8.05 eV [26], which is not accessible with two 337 nm photons from the N<sub>2</sub> laser that is commonly employed in UV-MALDI. They also present arguments against classical excited-state proton transfer for primary ion formation from this matrix. They suggest two-center processes as prime candidates for explaining UV-MALDI, such as energy pooling and subsequent photo/thermal ionization [26]. A related possible mechanism is energy pooling followed by a matrix disproportionation reaction, yielding a pair of protonated and deprotonated matrix

Table 2

Results from modified bracketing experiments. Literature values from Ref. [24] were obtained from ion/molecule equilibrium measurements

$(M-H)^-$ derived from	GB( $(M-H)^-$ ) [kJ/mol]	literature value [kJ/mol]
3-aminoquinoline 	1450.7 ± 11.5	–
<i>para</i> -aminophenol 	1438.3 ± 11.5	1450 ± 8.4*
<i>para</i> -nitroaniline 	1410.6 ± 11.5	1407 ± 8.4*
2-amino-5-nitropyridine 	1398.8 ± 11.5	–
2-amino-3-hydroxypyridine 	1398.5 ± 11.5	–
4-hydroxybenzoic acid 	1378.0 ± 11.5	1376 ± 8.4*
nicotinic acid 	1365.5 ± 11.5	–
3-hydroxypicolinic acid 	1365.3 ± 11.5	–
2,5-dihydroxybenzoic acid 	1329.4 ± 11.5	–
2,4,6-trihydroxyacetophenone 	1324.3 ± 7.1**	–

\* From [24].

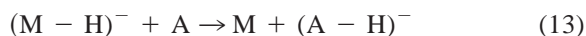
\*\* See text.

ions. With GB values of neutral matrix molecules from the literature and the data reported here, the energy required for a ground-state matrix disproportionation reaction can now be calculated.

Nicotinic acid, 3-hydroxypicolinic acid, 2,5-dihydroxybenzoic acid, and 2,4,6-trihydroxyacetophenone were reported to have proton affinities of 904 [6,9], 895 [6,7], 853 [7–9], and 882 kJ/mol [7], respectively. We estimate the corresponding GBs to be about 30 kJ/mol lower, which is the typical entropy contribution at 300 K [25]. It follows that the difference in GBs of neutral and anionic matrix species is about 492, 500, 506, and 472 kJ/mol, respectively. The energy required for a proton disproportionation reaction between two matrix molecules is then roughly 5 eV, which is much less than two 337 nm photons.

## 5.2. Oligonucleotide analysis

An analyte class which is predominantly detected in negative polarity is that of nucleic acid oligomers [27]. In typical negative ion MALDI mass spectra, oligonucleotides appear as deprotonated molecules which can result from a deprotonation reaction with matrix anions via reaction (13),



where A is the analyte and M is the matrix molecule. Reaction (13) proceeds towards products if  $\Delta GB < 0$  ( $\Delta GB = GB((A - H)^-) - GB((M - H)^-)$ ).

Gas-phase basicities of deprotonated oligonucleotides have not yet been determined and are the subject of current investigations. However, in laser desorption/chemical ionization experiments, an adenosine-5'-monophosphate (AMP) anion proton affinity of about 1280 kJ/mol was derived from unimolecular dissociation analysis [23]. The GB of  $(AMP - H)^-$  should be about 30 kJ/mol lower, because of the typical entropy contribution at 300 K [25]. Because all nucleic acids are identical with respect to their acidic function, the phosphate group, oligonucleotide GBs should not differ largely from this value, 1250 kJ/mol.

Matrix anion GBs were found to lie between 1324

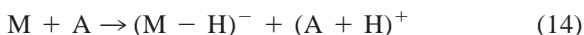
and 1451 kJ/mol, significantly higher than the estimated oligonucleotide anion GB in all cases. Therefore, with all matrices investigated here, a ground-state oligonucleotide deprotonation via reaction (13) is energetically favorable.

In order to avoid or minimize analyte fragmentation, the excess energy released in an exoergic deprotonation reaction should be kept as small as possible, meaning that the differences in matrix and analyte anion GBs should be small. For oligonucleotides, a "soft" deprotonation reaction occurs if the GB of the matrix anion is higher than, but close to the GB of the nucleotide anion ( $GB \approx 1250$  kJ/mol). The GB of the THAP anion is closest to the estimated value ( $\Delta GB \approx -75$  kJ/mol), and from the point of view of chemical ionization and neglecting excited state chemistry, it constitutes the softest reagent anion for oligonucleotide deprotonation found here. The next least basic anion is that of DHB ( $\Delta GB \approx -80$  kJ/mol). The 3-hydroxypicolinic acid (HPA) anion basicity is about 40 kJ/mol higher ( $\Delta GB \approx -115$  kJ/mol). HPA should still be a good candidate for soft nucleotide deprotonation because activation energies for dinucleotide anion fragmentation were measured to be about 120 kJ/mol [28].

This is consistent with experimental findings. THAP [29] and HPA [30] were found particularly suitable for nucleic acid analysis in negative ion mode. Both matrix anions are located on the lower end of the basicity scale, which is in agreement with the above considerations. Tang and co-workers found that DHB is a good matrix for short oligonucleotides up to 5 bases in negative ion mode, but for larger oligomers composed of 15 mixed bases, strong fragmentation was observed [31]. Moreover, for larger oligonucleotides, the DHB induced more fragmentation than HPA in negative mode [32]. The results for small oligonucleotides are consistent with the thermodynamic considerations, but a thermodynamic explanation fails for larger oligonucleotides. Zhu and co-workers suggest that the observed fragmentation is initiated by protonation of the nucleic acid bases, followed by base loss and phosphodiester backbone cleavage [32]. In this complex, multi-step process, the ability of a matrix to protonate the bases should

therefore be a key factor for the observed fragmentation in negative ion mode. Because the proton affinity of DHB is 853 kJ/mol, 42 kJ/mol lower than that of HPA, their model can be used to explain the observed stronger fragmentation in the case of DHB when compared to HPA. However, it is not clear why this mechanism only contributes when analyzing larger oligonucleotides.

It was also suggested that analyte molecules can be ionized by a ground state proton transfer from neutral matrix molecules, yielding protonated analyte and deprotonated matrix [33], as in reaction (14):



Reaction (14) is exoergic if  $GB(A) > GB((M - H)^-)$ . The matrix anion GBs found here clearly show that a ground state mechanism is energetically unfavorable and can generally be excluded. The gas-phase basicities of adenosine, cytidine, guanosine, and thymidine are 956.8, 950, 960.9, and 915.9 kJ/mol, respectively [24]. Because the bases are the site of protonation in oligonucleotide MALDI [31], we estimate the GBs of mixed base oligonucleotides to be roughly 955 kJ/mol. A proton disproportionation reaction of oligonucleotides with GBs not exceeding 1000 kJ/mol and a matrix anion is endoergic by at least 300 kJ/mol. In general, for a proton disproportionation reaction between analyte and matrix to occur, an analyte basicity of at least 1300 kJ/mol is required. Only very few substances with GBs higher than 1000 kJ/mol have yet been found, such as sodium hydride (GB = 1070 kJ/mol) and disodium oxide (GB = 1345 kJ/mol) [24]. The highest GB of an organic molecule reported is that of  $(CH_3)_2NC(CH_3) = N - (CH_2)_3N(CH_3)_2$  (GB = 1030 kJ/mol) [24], but even this strong base is not able to abstract protons from neutral matrix molecules. These reactions might become energetically favorable if the matrix anion GB is lowered as it can be the case in an electronically excited state. However, the change in GB upon electronic excitation would have to be on the order of 300 kJ/mol, which does not seem likely. Calculated differences in GBs of

excited and ground state were at most 200 kJ/mol and generally much lower [34].

Ammonium salts have become important as comatrices in oligonucleotide MALDI mass spectrometry, among them ammonium acetate [35] and ammonium fluoride [36]. Zhu and co-workers suggest that besides suppressing alkali-ion adducts, ammonium salts have both a protonation and deprotonation function [37]. It was recently shown that in a laser desorption/chemical ionization deprotonation reaction, the acetate and fluoride anions cause substantial fragmentation of the relatively fragile nucleotides [23]. We therefore think it is unlikely that ammonium acetate or fluoride should be potent deprotonation agents without inducing fragmentation at the same time. Li and co-workers did not observe fragmentation when using a HPA/ $NH_4F$  matrix [38]. Interestingly, they did observe fragmentation under the same conditions when using a 2A5NP/ $NH_4F$  matrix (see Fig. 4 in reference [38]). This is consistent with our data, because the 2A5NP anion GB is 1399 kJ/mol, 34 kJ/mol higher than that of HPA, making the deprotonation reaction exoergic with about 149 kJ/mol. Although ammonium salts are capable of improving the signal-to-noise ratio in MALDI mass spectra, we conclude that analyte ionization is controlled by the thermochemical properties of the MALDI matrix used. A possible alternative explanation for the observed signal enhancement is an improved incorporation of analyte molecules into the matrix crystals caused by the salt addition.

### 5.3. Peptide and protein analysis

MALDI analysis of peptides and proteins is usually performed in positive mode. However, with many matrices, MALDI ion generation is possible in negative polarity as well as in positive polarity. The gas-phase basicities of deprotonated  $\alpha$ -amino acids have been determined by O'Hair et al. to lie between 1356 kJ/mol (histidine) and 1402 kJ/mol (glycine) [39]. Deprotonated amino acid side chain proton affinities were estimated to range from 1439 kJ/mol to above 1632 kJ/mol, corresponding to GBs of about 1409 and 1602 kJ/mol, respectively [40]. With these data, we can estimate the GBs of deprotonated pep-

tides and proteins to lie between 1356 and 1402 kJ/mol. Depending on the peptide or protein composition, a ground-state deprotonation reaction of the type shown in Eq. (13) is energetically favorable with a variety of matrix anions, especially with the more basic ones.

As for the oligonucleotides, it can be shown that a disproportionation reaction of the type shown in Eq. (14) between peptides or proteins and neutral matrix is energetically unfavorable. The proton affinities of  $\alpha$ -amino acids have been measured [41–43], from which gas-phase basicities between 830 and 1000 kJ/mol can be derived. Gorman and Amster determined the gas-phase basicities of dipeptides that contain valine to be at most 960 kJ/mol [44]. These data suggest peptide and protein GBs generally not higher than 1000 kJ/mol, making the reaction endergic by at least 300 kJ/mol.

## 6. Conclusions

Laser desorption of preformed reference ions from a binary liquid/solid matrix was found to be a unique and effective method in FTICR bracketing experiments. In many cases near-equilibrium conditions were established, allowing us to fit the data to a function derived from equilibrium theory, and thereby extract the gas-phase basicities of the matrix anions. The method was validated by equilibrium-bracketing three anions with known gas-phase basicity. Good agreement with literature values was found. The results show substantial differences among the various matrix anions, whose basicities span an energy range of 127 kJ/mol, or 1.3 eV. Matrix–matrix disproportionation reactions were found to be energetically accessible with two 337 nm photons, and the energies required can be estimated to be about 5 eV. The derived matrix GB values were used to evaluate analyte deprotonation mechanisms, which are discussed in detail for oligonucleotides. Analyte deprotonation via matrix anions was found to be energetically favorable, whereas a proton disproportionation reaction between neutral matrix and analyte can be excluded.

## Acknowledgement

The authors thank the Kommission für Technologie und Innovation (KTI, grant no. 3165.1) for financial support.

## References

- [1] M. Karas, D. Bachmann, U. Bahr, F. Hillenkamp, *Int. J. Mass Spectrom. Ion Processes* 78 (1987) 53.
- [2] H. Ehring, M. Karas, F. Hillenkamp, *Org. Mass Spectrom.* 27 (1992) 472.
- [3] R. Knochenmuss, V. Karbach, U. Wiesli, K. Breuker, R. Zenobi, *Rapid Commun. Mass Spectrom.* 12 (1998) 529.
- [4] V. Bökelmann, B. Spengler, R. Kaufmann, *Eur. Mass Spectrom.* 1 (1995) 81.
- [5] G.R. Kinsel, R.D. Edmonson, D.H. Russel, *J. Mass Spectrom.* 32 (1997) 714.
- [6] T.J.D. Jørgensen, G. Bojesen, H. Rahbek-Nielsen, *Eur. Mass Spectrom.* 4 (1998) 39.
- [7] C.M. Nelson, K. Crellin, J. Berry, J.L. Beauchamp, L.M. Smith, *Proceedings of the 44th ASMS Conference on Mass Spectrometry and Allied Topics*, edited by A.B. Giordani, Portland, 1996, p. 733.
- [8] R.J.J.M. Steenvoorden, K. Breuker, R. Zenobi, *Eur. Mass Spectrom.* 3 (1997) 339.
- [9] R.D. Burton, C.H. Watson, J.R. Eyler, G.L. Lang, D.H. Powell, M.Y. Avery, *Rapid Commun. Mass Spectrom.* 11 (1997) 443.
- [10] A.G. Harrison, *Mass Spectrom. Rev.* 16 (1997) 201.
- [11] D.K. Bohme, R.S. Hemsworth, H.W. Rundle, H.I. Schiff, *J. Chem. Phys.* 58 (1973) 3504.
- [12] S.A. McLuckey, D. Cameron, R.G. Cooks, *J. Am. Chem. Soc.* 103 (1981) 1313.
- [13] J.L. Wilbur, B.D. Wladkowski, J.I. Braumann, *J. Am. Chem. Soc.* 115 (1993) 10 823.
- [14] R.C. Dunbar, T.B. McMahon, *Science* 279 (1998) 194.
- [15] J.L. Beauchamp, S.E. Buttrill, *J. Chem. Phys.* 48 (1968) 1783.
- [16] G. Bouchoux, J.Y. Salpin, D. Leblanc, *Int. J. Mass Spectrom. Ion Processes* 153 (1996) 37.
- [17] J. Wu, C.B. Lebrilla, *J. Am. Soc. Mass Spectrom.* 6 (1995) 91.
- [18] J.W. McKiernan, C.E.A. Beltrame, C.J. Cassidy, *J. Am. Soc. Mass Spectrom.* 5 (1994) 718.
- [19] T. Su, M.T. Bowers, *Int. J. Mass Spectrom. Ion Phys.* 12 (1973) 347.
- [20] I.J. Amster, D.P. Land, J.C. Hemminger, R.T. McIver, *Anal. Chem.* 61 (1989) 184.
- [21] P.W. Atkins, *Physical Chemistry*, Fifth ed., Oxford University Press, Oxford, 1995.
- [22] A.G. Harrison, *Chemical Ionization Mass Spectrometry*, 2nd Edition, CRC, Boca Raton, 1992.
- [23] K. Breuker, R. Knochenmuss, R. Zenobi, *Int. J. Mass Spectrom. Ion Processes* 176 (1998) 149.
- [24] J.E. Bartmess, “Negative Ion Energetics Data” in NIST

- Standard Reference Database Number 69, W.G. Mallard, P.J. Linstrom (Eds.), August 1997, National Institute of Standards and Technology, Gaithersburg MD, 20899 (<http://webbook.nist.gov>).
- [25] G.L. Lias, J.E. Bartmess, J.F. Liebmann, J.L. Holmes, R.D. Levin, W.G. Mallard, *J. Phys. Chem. Ref. Data* 17 (1988) 1 (suppl).
- [26] V. Karbach, R. Knochenmuss, *Rapid Commun. Mass Spectrom.* 12 (1998) 968.
- [27] E. Nordhoff, F. Kirpekar, P. Roepstorff, *Mass Spectrom. Rev.* 15 (1996) 67.
- [28] M.T. Rodgers, S. Campbell, E.M. Marzluff, J.L. Beauchamp, *Int. J. Mass Spectrom. Ion Processes* 137 (1994) 121.
- [29] U. Pieleles, W. Zürcher, M. Schär, H.E. Moser, *Nucl. Acids Res.* 21 (1993) 3191.
- [30] K.J. Wu, A. Steding, C.H. Becker, *Rapid Commun. Mass Spectrom.* 7 (1993) 142.
- [31] W. Tang, C.M. Nelson, L. Zhu, L.M. Smith, *J. Am. Soc. Mass Spectrom.* 8 (1997) 218.
- [32] L. Zhu, G.R. Parr, M.C. Fitzgerald, C.M. Nelson, L.M. Smith, *J. Am. Chem. Soc.* 117 (1995) 6048.
- [33] R.C. Beavis, T. Chaudhary, B.T. Chait, *Org. Mass Spectrom.* 27 (1992) 156.
- [34] L.W. Sumner, Y. Huang, D.H. Russel, *Proceedings of the 44th ASMS Conference on Mass Spectrometry and Allied Topics*, A.B. Giordani (Ed.), Portland, 1996, p. 271.
- [35] G.J. Currie, J.R. Yates, *J. Am. Soc. Mass Spectrom.* 4 (1993) 955.
- [36] S. Cheng, T.D. Chan, *Rapid Commun. Mass Spectrom.* 10 (1996) 907.
- [37] Y.F. Zhu, N.I. Taranenko, S.L. Allman, S.A. Martin, L. Haff, C.H. Chen, *Rapid Commun. Mass Spectrom.* 10 (1996) 1591.
- [38] Y.C.L. Li, S. Cheng, T.D. Chan, *Rapid Commun. Mass Spectrom.* 12 (1998) 993.
- [39] R.A.J. O'Hair, J.H. Bowie, S. Gronert, *Int. J. Mass Spectrom. Ion Processes* 117 (1992) 23.
- [40] E.M. Marzluff, S. Campbell, M.T. Rodgers, J.L. Beauchamp, *J. Am. Chem. Soc.* 116 (1994) 7787.
- [41] G.S. Gorman, J.P. Speir, C.A. Turner, I.J. Amster, *J. Am. Chem. Soc.* 114 (1992) 3986.
- [42] M. Meot-Ner, E.P. Hunter, F.H. Field, *J. Am. Chem. Soc.* 101 (1979) 686.
- [43] M.J. Locke, R.T. McIver, *J. Am. Chem. Soc.* 105 (1983) 4226.
- [44] G.S. Gorman, I.J. Amster, *J. Am. Chem. Soc.* 115 (1993) 5729.